Efficient Determination of Misalignment of Ladle Shroud Using Machine Vision

Digital technologies are transforming industry at all levels. Steel has the opportunity to lead all heavy industries as an early adopter of specific digital technologies to improve our sustainability and competitiveness. This column is part of AIST's strategy to become the epicenter for steel's digital transformation, by providing a variety of platforms to showcase and disseminate Industry 4.0 knowledge specific for steel manufacturing, from big-picture concepts to specific processes.



Authors

Arijit Das (top row, left)
lead engineer — automation and control, M.N. Dastur & Co. (P) Ltd., Kolkata, India
arijit.das@dastur.com

Saikat Chatterjee (top row, right)
principal consultant, Dastur Innovation Labs, Toronto, Ont., Canada
chatterjee.saikat@dastur.com

Atanu Mukherjee (bottom)
president and chief executive officer, M.N. Dastur & Co. (P) Ltd., Kolkata, India
atanu.m@dastur.com

Continuous casting of steel includes multiple transfer operations of liquid steel from ladle to mold via the tundish, followed by its solidification to semi-finished products such as blooms, billets or slabs. Since the transfer operations can easily result in the reoxidation of liquid steel, it presents significant challenges in terms of retaining the steel quality obtained through secondary metallurgical operations such as ladle refining, vacuum degassing or RH degassing. Over the years, transfer operations have seen significant improvement due to increased usage of slidegates, ladle shrouds, ladle nozzles, and flow modifiers such as impact pads, weirs, dams and so on.[1] Injection of inert gases into the ladle shroud has also turned out to be a common practice as it creates a protective gas blanket that prevents air ingress and subsequent reoxidation.

Although much has been done to improve the process, one aspect of transfer operation that has largely gone unnoticed is the misalignment of the ladle shroud. On careful observation, it can be noticed that the ladle shroud becomes tilted with respect to the vertical direction. Recently, Chattopadhyay et al.[2] and Chatterjee et al.[3] have pointed out continuous casting operations in both billet caster and slab caster with misaligned ladle shrouds, as depicted in Fig. 1. The luminous circular regions and dark cylindrical regions depict tundish open eyes (TOEs)[3] and ladle shrouds, respectively. Ladle shroud misalignment affects steel quality and operation as it undermines the performance of impact pad and dams, causing adverse flow conditions, increasing the chance of open eye formation and decreasing the residence time for inclusion flotation along with increasing refractory wear in continuous casting.[3]

Physical Description of the Problem

Possible Causes of Shroud Misalignment

— During continuous casting operations, the ladle turret swivels and the empty ladle is replaced by a filled ladle. The ladle shroud is then placed on the collector plate nozzle,

Figure 1

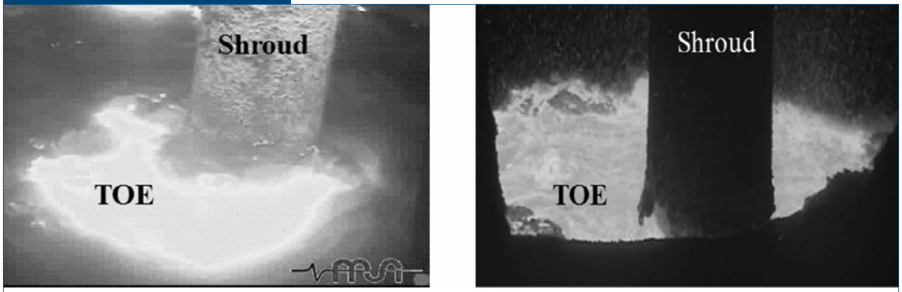

(a) (b)

Photographs showing misaligned ladle shrouds during plant operations resulting in the formation of eccentric tundish open eyes (TOE) in a billet caster (a) and a slab caster tundish (b).[3]

Figure 2

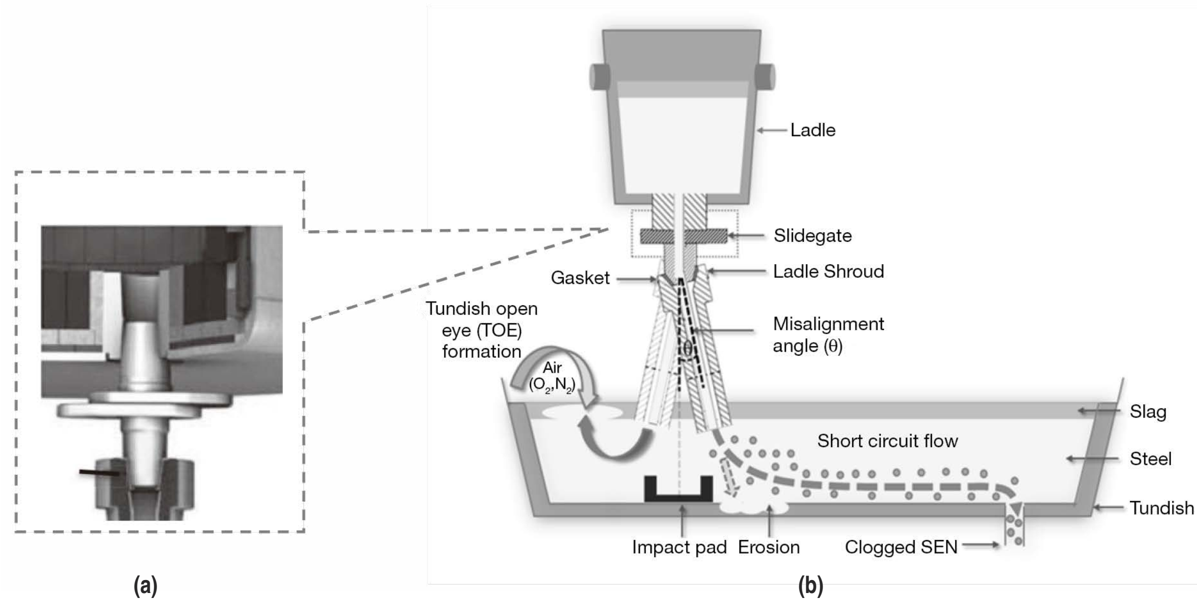

Mounting of an actual shroud on a collector plate nozzle (a)[1] and schematic representation of shroud misalignment (exaggerated view) and its effect on steel quality (b).

at the ladle bottom. The sheer inertial force generated due to the flow of liquid steel within the ladle, or within the shroud, can easily displace or incline the shroud from its intended position. A schematic diagram of the ladle bottom collector plate/ladle shroud assembly is depicted in Fig. 2a.

Steel plant operators often clean the inclusions/solid residue sticking on the inner walls of a ladle shroud by blowing a supersonic oxygen jet just before attaching the shroud to the collector nozzle. Many times, all of the residue is not removed due to improper blowing of oxygen jet and, as a result, the inner surface of the shroud becomes uneven, which can result in improper setup of the whole arrangement. The ladle shroud can easily become misaligned when it is being fixed to the ladle bottom.

Effect of Shroud Misalignment on Steel Quality — A schematic representation of misaligned shrouded transfer of molten steel from ladle to tundish along with other associated events is depicted in Fig. 2b.

Flow control devices (FCDs) such as turbo-stop, weirs and dams are usually placed inside the tundish in order to obtain clean steel by aiding inclusion flotation to the top surface. The inclusions are then collected by the overlying slag layer. The recirculatory flows within the tundish, along with the buoyancy effect, help in inclusion flotation. The main objective of these FCDs is to restrain the flow of highly turbulent liquid steel within itself, which prevents the spread of incoming inclusions throughout the whole tundish. The entrainment of inclusions into the mold via the submerged entry nozzles (SENs) is thus prevented. However, confining the highly turbulent flow within the turbo-stop region becomes more and more difficult if the misalignment of the ladle shroud increases. The inclination of the ladle shroud on a particular side directs the fluid flow in a path away from that which was intended. The residence time, which is defined as the time a single fluid element spends in the tundish, decreases due to much reduced recirculatory flows and hence results in reduced inclusion flotation. The negative effects of shroud misalignment can be stated as follows:

- Tundish bottom refractory life reduction: The flow directed outside the turbo-stop results in increased wear/erosion of the tundish bottom refractory. The maintenance cost thus increases due to increased gunning of refractory mass at the tundish bottom.
- SEN life reduction: Biased flow of inclusions toward the SEN may result in its increased clogging, thus necessitating its premature replacement.
- Eccentric open eye: A misaligned ladle shroud in a particular direction can lead to formation of an eccentric open eye in the corresponding direction,[3] giving rise to reoxidation and quality issues. Reoxidation of steel occurs when it comes into direct contact with ambient air. Harmful inclusions such as Al_2O_3,[4] Al_2O_3-TiOx[5] or $MnAl_2O_4$[6] can form when oxygen and nitrogen present in air react with dissolved

elements in steel such as Al, Mn and Ti. These inclusions have a tendency to form clusters and attach to the walls of the nozzles, thereby clogging them.
- Product quality deterioration: Inclusions that pass on to the final product can be very detrimental to the product quality, severely affecting mechanical properties such as fatigue and fracture toughness.[7,8]

A couple of recent studies[3] show the effect of ladle shroud misalignment on fluid flow within the tundish. From the calculated turbulent kinetic energy contours within a slab caster tundish for different cases of misalignment, viz. 0°, 2° and 5°, Chatterjee and Chattopadhyay[3] observed that the turbulent flow from the shroud shifts away from its intended target with increasing misalignment angle. As can be observed from Fig. 3, although the flow for the case of 2° misalignment can still be confined within the turbo-stop region, the same is not true for the case of 5° misalignment.

Since the inclusion trajectories follow the path of fluid flow in the tundish, they can be easily dispersed into the bulk liquid steel or flow preferentially toward the direction of bias, instead of floating up to the overlying slag layer. Chattopadhyay et al.[2] performed physical modeling experiments with 5° misalignment in a billet caster tundish to see its effect on inclusion dispersion within the bulk fluid. It was clearly observed that more slag droplets (polyethylene beads) were entrained in the direction of misalignment, as depicted in Fig. 4. These experimental observations strongly substantiate the claims previously mentioned.

Machine Vision Approach

The artificial intelligence (AI) and Industrial Internet of Things (IIoT) integrate production technology and information technology to support smart factories across the globe. Over the years, various approaches have been used to provide customized solutions for steel productivity improvement. Among them, the machine vision approach, instead of manual inspection, improves quality enhancement by image-based automatic inspection, component monitoring and analysis from raw materials to final product. Machine vision comprises several stages: image acquisition, processing, segmentation and recognition. Several successful practical applications of machine vision in the steel industry have been reported in the past, including:

- Slag detection system.[12,13]
- Coil surface defect detection.[14,15]
- Blast furnace tuyere monitoring system.[16,17]
- Refractory maintenance.[18,19]

Rationale for Machine Vision — Machine vision (MV) provides automatic recognition and evaluation of images for automatic inspection, process control

Figure 3

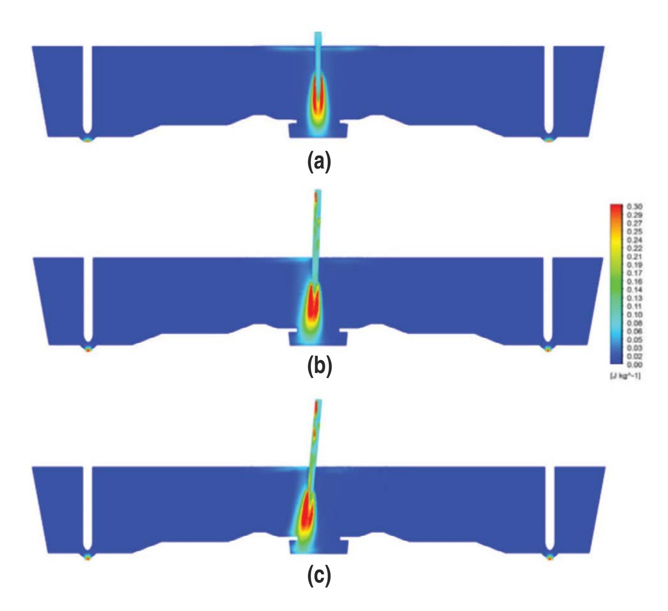

Turbulent kinetic energy contours inside tundish at a misalignment angle of: 0° (a), 2° (b) and 5° (c).[3]

Figure 4

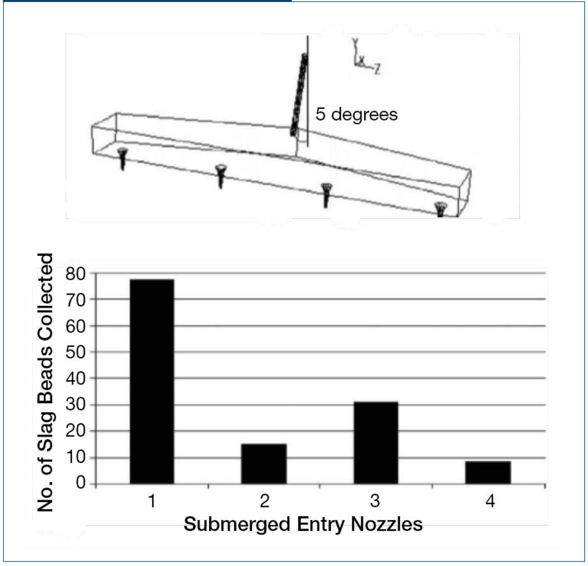

Preferential inclusion entrainment in the direction of misalignment.[2]

and robot path guidance in industry. An MV system consists of (a) vision camera for object detection and (b) computer vision algorithms for feature extraction, image analysis and quantitative measurement. The relative advantages of an MV system as compared to other possible sensor systems (such as infrared, laser, ultraviolet) for shroud misalignment detection are as follows:

- Lower capital cost compared to a system consisting of infrared/laser sensor array along with their logic controllers.
- Multiple feature extraction including object shape, pattern, color and geometry recognition.
- Different types of foreground separation techniques can be applied depending on the environmental hazards.
- Several kinds of electromagnetic radiation, such as radio waves, infrared, ultraviolet and gamma radiation, which lead to error of the measured variable, can be avoided.
- Higher-resolution cameras provide pixel spreading over a large surface area lead to higher degree of precision.
- Better speed of response, accuracy, reliability and repeatability.
- Two connection points are sufficient between the camera and central processor unit without any signal conditioning.
- Flexibility of the object 3D rendering leads to proper investigation and visualization of the system.

Stereo Vision

Stereo vision is an area of study in the field of machine vision that recovers 3D information of an object using two or more images from camera. The depth output of each pixel is determined by computing the difference of two pixel positions in two different image planes. Finally, the disparity map is obtained by filling the spaces between two consecutive edge pixels. In short, it emulates the human vision by using two or more 2D views of the same view to derive its 3D depth information.

An efficient stereo vision algorithm was developed to reliably detect shroud misalignment by deriving its 3D depth information from captured 2D images. Extensive experiments were conducted to demonstrate that this approach can provide consistent results in misalignment detection. In the present work, a simplified stereo vision technique is depicted in Figs. 6 and 7. Stereo vision fundamentally works on the principle of triangulation.[9]

Figure 5

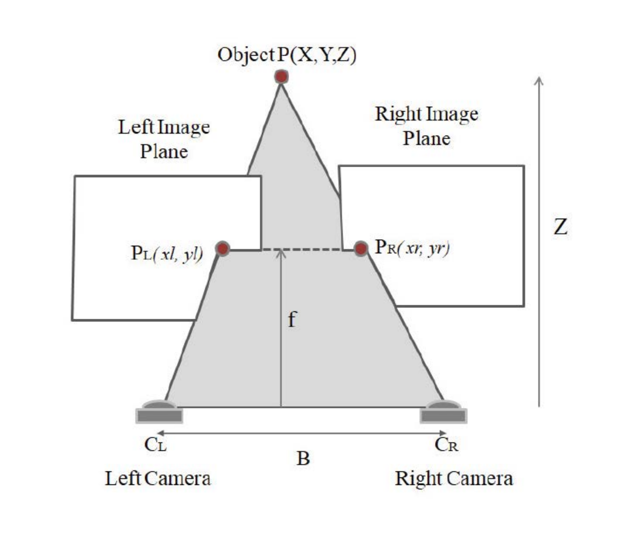

Schematic representation of the triangulation technique.

Fundamental Principle of Stereo Vision — Triangulation is a robust technique that facilitates verification of data through cross-verification from two or multiple sources. The stereo vision technique refers to the process of determining a 3D space given its projection onto two or more images.

Using a pair of stereo images, the apparent pixel difference of a particular pixel, cell or patch can be calculated. This is called the disparity, which is depicted in Fig. 5. The values in this disparity map are inversely proportional to the scene depth at the corresponding pixel location. Disparity mapping allows for the computation of depth map information.

Points C^L, C^R and P (and P^L and P^R) lie on a plane. Since two image planes lie on the same plane (distance f from each camera), the lines C^LC^R and P^LP^R are parallel. The distance between the centers of the two lenses is called the baseline width (B), focal length (f) and disparity (D). The projection of the world point on the two image planes is (xl, yl) and (xr, yr). So, the following equation was obtained from the method of similarity of triangles:[9]

$$\text{Depth } (Z) = f * B / D \tag{Eq. 1}$$

Proposed Methodology

In the proposed model, two web cameras have been used with their optical axes parallel and aligned horizontally. The disparities of 3D points mapped to pixels in two images are computed by using the principle of triangulation. Its essence is to schematically reconstruct a 3D object (pipe) by analyzing the 2D information extracted. The deviation of angle with reference to a vertical line in 3D geometry can be acquired using these disparities.

Proposed Hardware Design and Implementation — The proposed system consists of a couple of cameras (30 fps @640X480, 60° FOV) where the optical axes are parallel. This is used to get two different images (left and right) in a manner similar to human binocular vision placed at a distance from a sphere-shaped pipe. A hollow PVC pipe with proper high-intensity LED radiation generates a function simulating the shroud that can be aligned at different angles in different quadrants through a mechanical ball joint arrangement shown in Figs. 6 and 7.

Software Design — By enhancing the image processing algorithm and disparity computation method, the misalignment angle of the shroud was estimated, along with a relative 3D schematic reconstruction from the relative disparity point calculation. A simple block diagram of the system is shown in Fig. 8.

In this application, a setup of OpenCV (Open Source Computer Vision Library) in the Ubuntu operating system has been employed to obtain the flexibility of image captures directly from the camera and use its library programming functions for image analysis. Code blocks is a cross-platform integrated development environment (IDE) to support compiling and running multiple languages. The complete algorithm is developed in the C++ environment.

For the epipolar rectified image pair, each point in the left image lies on the same horizontal line (epipolar line) as in the right image. This approach is used to reduce a search space for depth map computation algorithms. The depth of an image pixel is the distance of the corresponding space point from the camera center. To estimate the depth map and detect 3D objects, the corresponding pixels in the left and right images have to be matched. To eliminate significant distortion, camera calibration is mandatory, as shown in Fig. 9.

Stereo Rectification and Camera Calibration — In order to apply stereo ranging techniques with a higher level of accuracy, it is important to eliminate radial and tangential lens distortion, which gives extrinsic and intrinsic parameter by using a chess board (9 X 7 crossed) pattern. The intrinsic parameters of individual camera include distortion coefficients and camera matrix (focal lengths and optical center).[10,11] Extrinsic coefficients contain information about rotation and translation matrices between the stereo pairs. Intrinsic parameters are used to remove the distortion in the image pairs and extrinsic parameters are then estimated with the help of corrected pairs. A few original image pairs of a chess board, considered for camera calibration, are shown in Fig. 9. The following data are obtained from the camera calibration algorithm:[10,11]

- The camera matrix (intrinsic and extrinsic parameter).
- The distortion matrix.

Figure 6

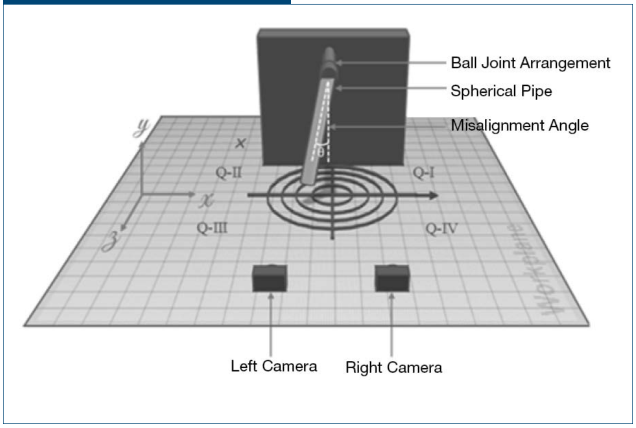

Front view of the proposed 3D model.

Figure 7

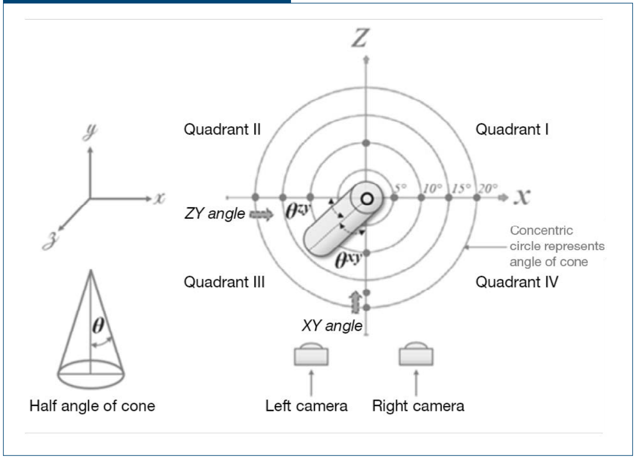

Top view of the proposed 3D model.

Algorithm of the Proposed System

On-Line Frame Capturing: Image capturing is a fundamental step in machine vision to prepare raw data. By creating a video capture application programming interface (API), the left and right images are simultaneously captured frame by frame.

Distortion Rectification/Remapping: Raw image frames can be rectified by several linear and non-linear

Figure 8

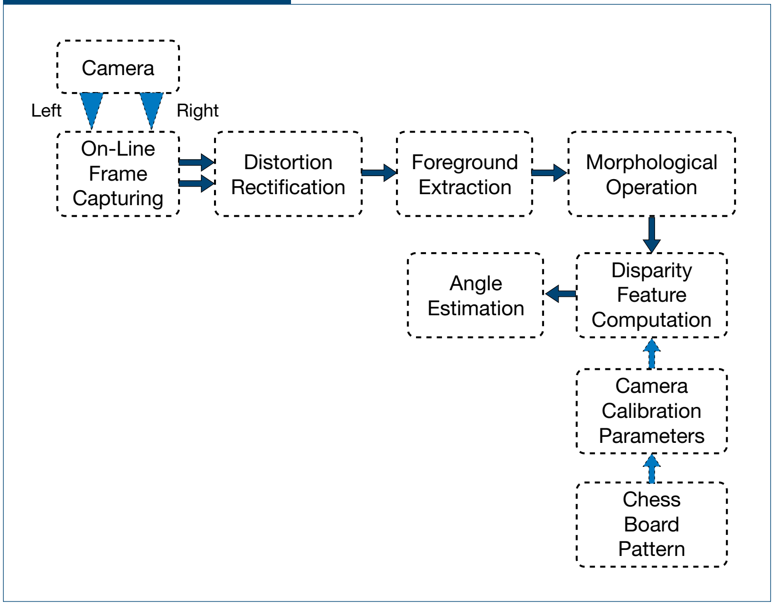

System flow chart diagram.

Figure 9

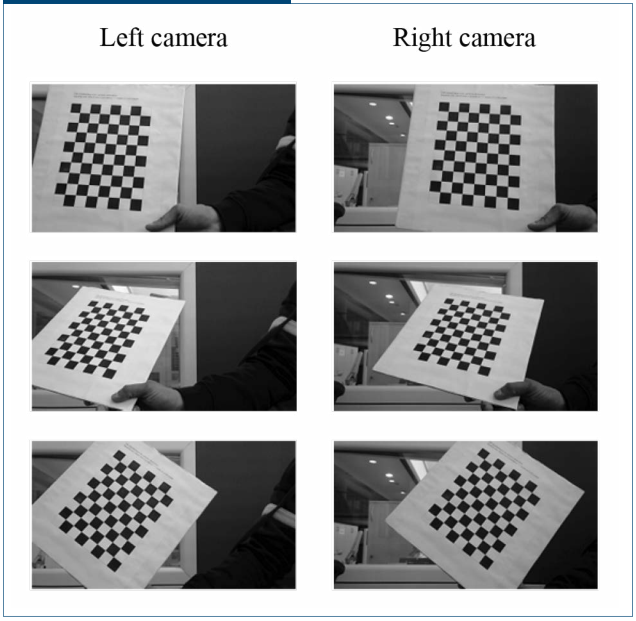

Original image pairs of a chess board captured for camera calibration.

techniques for 2D images. The image content is not changed but the pixel grid is deformed and mapped to the destination image. The computed response is stored in the destination image at the same location (x, y). It means that the output image is the same size as the input image. Prior to image rectification, it is essential to choose a valid region of interest (ROI) by the upper and lower threshold limits with a variable track bar method.

Foreground Extraction: Prior to the rectification of the valid image, the foreground (i.e., pipe) is extracted from the background object, which may vary depending upon the steel structure. There are different types of background foreground segmentation methods such as GrabCut-based segmentation, superpixel-based segmentation, watershed-based segmentation, etc. The method of implementation of segmentation algorithm can be chosen depending on the type of actual environment. In this experimental model, HSV (hue, saturation, value) color space represents the color space similar to the RGB (red, green, blue) color model. By choosing the correct upper (HU) and lower (HL) boundaries' variation of the different hue value, the red-hot pipe is filtered out or separated from the background. For industrial noisy environments, the process of segmentation may differ but can be used for any type of background foreground separation.

Morphological Operation: A morphological approach is used to decompose the object into simple components. After foreground extraction, multiple foreground or background noise bodies are removed by despeckling or the denoising filtration method. To precede this operation, a morphological opening and closing operation can be applied. Subsequently, a morphological technique is used here to preserve the structure of the shape but removes the entire identical pixel in order to achieve faster processing speed and a smaller memory footprint.

Feature Computation: The aim is to determine the relevant feature points in both the left and right image views of the pipe. In this particular case, the feature of the pipe is well defined and statistically sound rather than being statistically fuzzy. So the feature computation technique of the particular system is fairly straightforward. Various appropriate points were chosen, mainly top and bottom pixel points, to perform pixel matching between left and right image views. Ultimately by matching each pixel in the left image with its corresponding right image, the top disparity ($xl^{top} – xr^{top}$) and bottom disparity ($xl^{bot} – xr^{bot}$) are computed, as shown in Fig. 10.

Angle Estimation From 3D Geometry: The proposed methodology is used for detection of misalignment angle of the pipe with respect to its X and Z coordinates as the pipe lies in Y axis. The characteristic of the pipe is statistically sound and linear in nature, so dense disparity mapping is not required; rather a

Figure 10

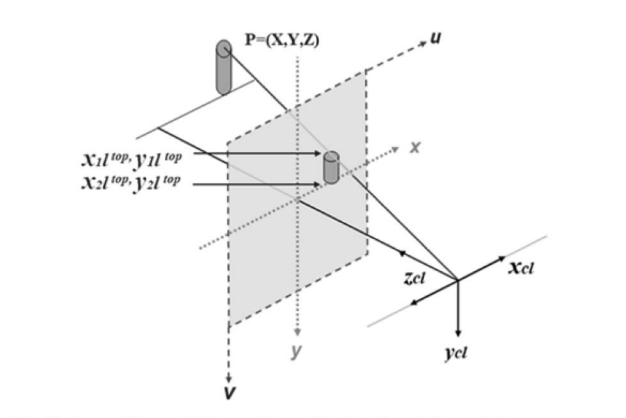

Disparity matching and depth calculation.

Table 1

Actual Angle (°) vs. On-Line Value

Actual XY angle (°)	On-line XY angle (°)	Deviation angle (°)	Actual ZY angle (°)	On-line ZY angle (°)	Deviation angle (°)
0	0.13	0.13	0	0.15	0.15
5	5.14	0.14	5	5.19	0.19
10	10.23	0.23	10	10.31	0.31
15	15.36	0.36	15	15.44	0.44
20	20.47	0.47	20	20.68	0.68

spark disparity method of two points is used. From the camera calibration method, the focal length (f) was already found. So, the final depth information (Z) is arrived at by using the camera intrinsic and extrinsic parameter and calculating the top depth (Z^{top}) and bottom depth (Z^{bot}) by Eqs. 2 and 3:

$$Z^{top} = f*b/(xl^{top} - xr^{top}) = f*b/d \qquad \text{(Eq. 2)}$$

$$Z^{bot} = f*b/(xl^{bot} - xr^{bot}) = f*b/d \qquad \text{(Eq. 3)}$$

Once the depth information is obtained, the conical X angle is computed with respect to Y coordinates and conical Z angle with respect to Y coordinates, which are the final measurement values for misalignment detection by the Pythagorean theorem, as shown in Eqs. 4 and 5:

$$\text{XY angle}\,(\theta^{xy}) = \tan^{-1} y/x \qquad \text{(Eq. 4)}$$

$$\text{ZY angle}\,(\theta^{zy}) = \tan^{-1} z/x \qquad \text{(Eq. 5)}$$

The measurement accuracy can be further improved by using a higher-resolution camera or increasing the camera base length.

Results and Discussion

In the experimental setup, a real angle-measuring arrangement was placed on both the backside of the plane and in the work plane (concentric circle) so that the measurement of the true angle of the misalignment can be visualized, as shown in Figs. 6

Figure 11

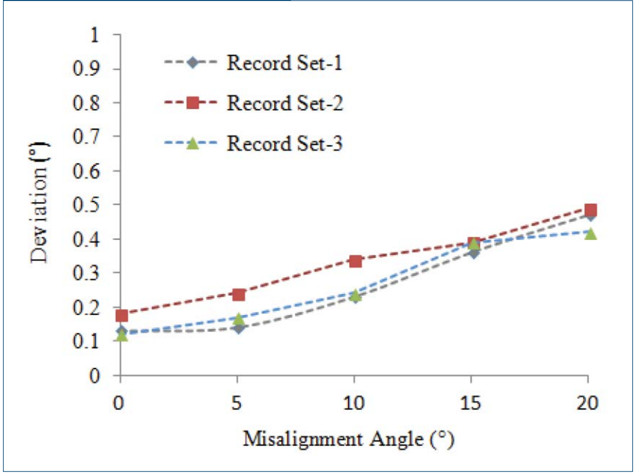

Deviation of actual XY angle with on-line value.

Figure 12

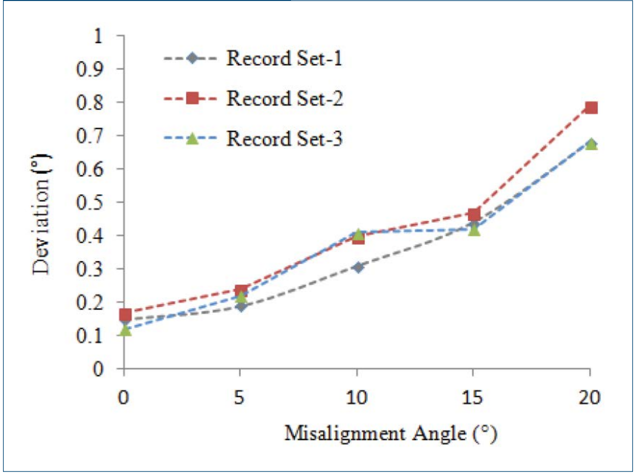

Deviation of actual ZY angle with on-line value.

Table 2

On-Line Monitoring Value for Different Angles With Different Quadrants

Quadrant	Image	On-line value
Vertical	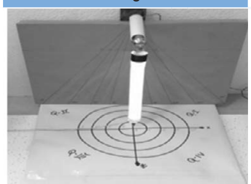	
QI	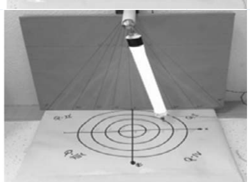	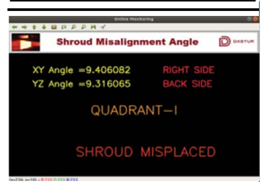
QII	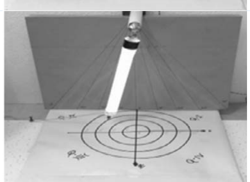	
QIII	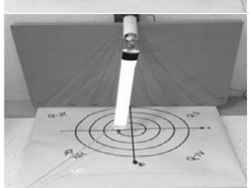	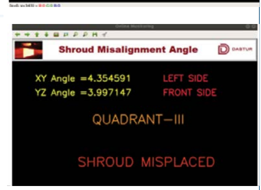
QIV	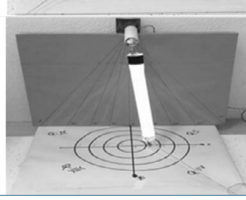	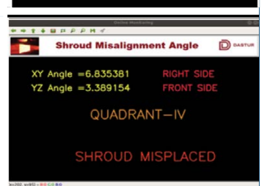

and 7. The shroud was placed at different angles in different quadrants and simultaneously actual and on-line angles were recorded, as shown in Table 2. A single data record set of θ^{xy} angle as well as the θ^{zy} angle for quadrant I are shown in Table 1. The errors of true value and measured value were also calculated. The proposed system was tested and verified by capturing multiple data record sets shown in Figs. 11 and 12. Based on the experiments, it was found that the final deviation of the value was within ±5%.

3D Rendering for On-Line Monitoring — To further monitor 3D widgets of the hollow pipe, VTK (visualization tool kit) was utilized, by using its volume rendering technique to obtain real-time on-line views of the pipe with reference to the 3D widget. The actual front view and the 3D reconstructed view of the misaligned pipe are shown in Figs. 13 and 14, respectively.

Shroud Misalignment Detection and Rectification System Setup in Plant Environment

Existing Setup and Operations — The existing plant operations employ a device called a "shroud manipulator," as shown in Fig. 15, to handle the ladle shroud in between transfer operations. A shroud manipulator is necessary as manual handling of red-hot ladle shrouds would be a major safety concern. However, the control of the shroud manipulator is in the hands of an operator, who regulates its movement using a joystick. It is very difficult for an operator to check the alignment of the ladle shroud with respect to the vertical axis after placing the ladle shroud in position, which can result in ladle shroud misalignment.

Corrective Action and Recommendations — The "integrated stereo vision system" developed in the present work is able to identify the alignment of the ladle shroud with an error of ±5%. An air-cooled water and dustproof housing (IP65/67) is required for it to sustain the hazardous industrial environment.

The raw image data from the stereo camera is first sent to the processing unit for interpretation and analysis using the custom-made image processing algorithm. The resulting misalignment angle is (a) revealed on a display monitor and (b) fed into a modular I/O controller, which can generate alarms when a pre-defined threshold value is attained. The shop floor personnel can take corrective actions when the threshold limit is crossed. This type of feedback control system has shown promising results in the plant environments and thus is well accepted in the steel industry.

Figure 13

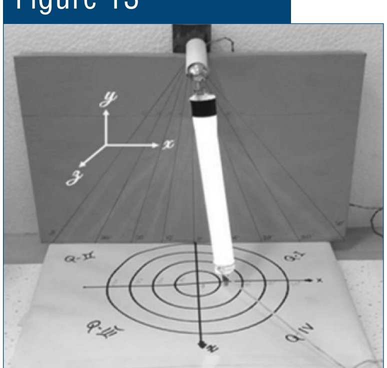

Front view of the pipe at particular angle.

Figure 14

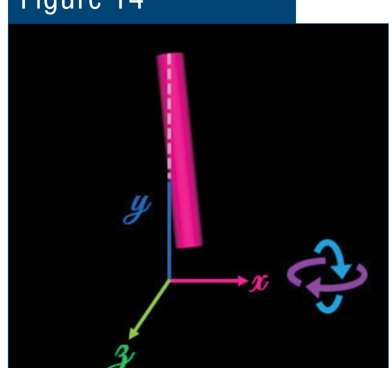

Schematic reconstruction of the pipe in 3D geometry.

Conclusion

Since ladle shroud misalignment results in various problems such as reduction in tundish bottom refractory life and SEN life, along with product quality deterioration on account of increased inclusion formation, on-line rectification is necessary. A machine vision approach has been developed to investigate the precise position of a ladle shroud and its angle of misalignment from the vertical axis. The integrated stereo vision system developed in the present work can be used during the continuous casting operation. The major advantages are as follows:

- Automatic and precise inspection system instead of manual visualization of the misalignment by the operator, thus enhancing productivity and quality.
- More cost-effective solution for caster operations compared to other sensors.
- Algorithm-based machine vision detection obviates the need for a graphics processing unit.
- Efficient denoising/despeckling image filtering algorithm increases precision in noisy environments.

The proposed method is a robust and cost-effective solution for detection of misalignment angle. Compared to other sensors, camera-based detection is a simpler solution and a simple computer vision algorithm technique can be used to get 3D correspondence of the shroud in a continuous caster. The computer vision algorithm used here also allows for super-resolution work. The algorithm used in the proposed system can also be embedded in a single-board computer system such as Raspberry Pi.

Future experiments will be conducted, along with tests for higher accuracy with a higher-resolution industrial camera and enhanced algorithms on a greater number of real (data) images with an aim to compare the presented approach with other existing algorithms. The reliability of the system will also be investigated by implementing it in very noisy operating environments.

Figure 15

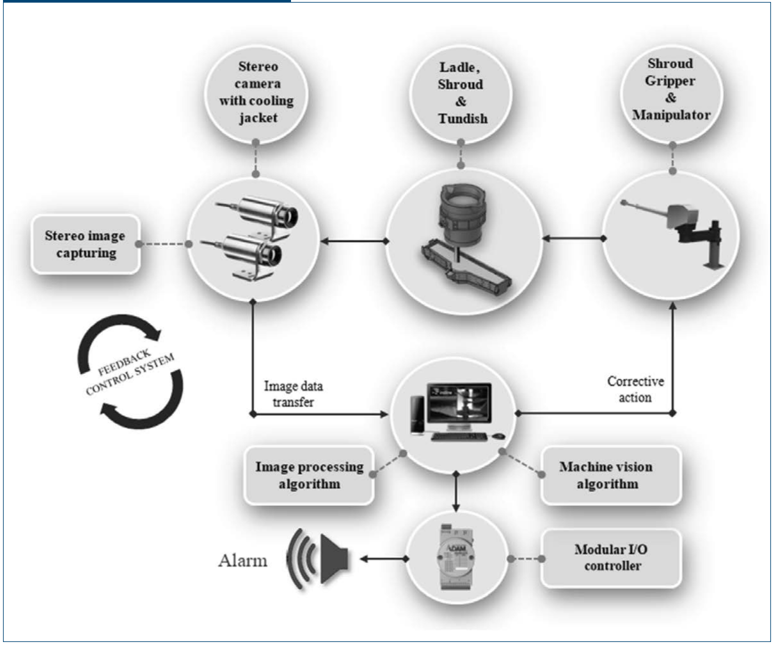

Schematic view of the plant setup for shroud misalignment detection.

References

1. D. Mazumdar, P.K. Singh and R.K.Tiwari, *ISIJ International,* Vol. 58, 2018, pp. 1545–1547.
2. K. Chattopadhyay, M. Isac and R.I.L. Guthrie, *ISIJ International,* Vol. 51, No. 5, 2011, pp. 759–768.
3. S. Chatterjee, D. Li and K. Chattopadhyay, *ISIJ International,* Vol. 56, 2016, pp. 1889–1892.
4. S. Chatterjee, Ph.D. thesis, University of Toronto, 2017.
5. C. Lyons and P. Kaushik, *Steel Research International,* Vol. 82, No. 12, 2011, pp. 1394–1403.
6. S. Chatterjee and I-H. Jung, *J. Eur. Cer. Soc.*, Vol. 34, No. 6, 2014, pp. 1611–1621.
7. K. Peaslee, V. Singh and S. Lekakh, *Proceedings of the Richard J. Fruehan Symposium,* 2011.
8. P.A. Thornton, *J. Mat. Sci.,* Vol. 6, 1971, pp 347–356.
9. https://docs.opencv.org/3.4.1/d0/dbd/group_triangulation.html.
10. http://www.cs.cmu.edu/~16385/s17/Slides/11.1_Camera_matrix.pdf.
11. https://tigerprints.clemson.edu/cgi/viewcontent.cgi?article=2216&context=all_theses.
12. https://www.vesuvius.com/en/our-solutions/sv-se/iron-and-steel/continuous-casting/ladle-to-tundish/slag-detection-systems.html.
13. https://www.ametek-land.com/products/fixedthermalimagersandlinescanners/sds-e.
14. http://automationtatasteel.com/html/SQIS.html.
15. http://www.winspection.com/surface-inspection.php.
16. http://automationtatasteel.com/html/tuyereye.html.
17. http://www.paulwurth.com/news-media/news-and-archives/market-breakthrough-for-tuyere-phenomena- detection-system.
18. http://www.tempsens.com/blog/thermal-imager/ladle-refractory-monitoring-system.
19. https://automationtechnology.de/cms/wp-content/uploads/2015/06/Ladle_Refractory_Monitoring_web.pdf. ✦

AISTech

This paper was presented at AISTech 2019 — The Iron & Steel Technology Conference and Exposition, Pittsburgh, Pa., USA, and published in the Conference Proceedings.